# A natural point mutation changes both target selectivity and mechanism of action of sea anemone toxins

**Steve Peigneur,* László Béress,[†,‡] Carolina Möller,[§] Frank Marí,[§] Wolf-Georg Forssmann,[†,‡] and Jan Tytgat*[,1]**

*Laboratory of Toxicology, University of Leuven (Katholieke Universiteit Leuven), Leuven, Belgium; [†]Department of Immunology and Rheumatology, Hannover Medical University, Hannover, Germany; [‡]Pharis Biotec GmbH, Hannover, Germany; and [§]Department of Chemistry and Biochemistry, Florida Atlantic University, Boca Raton, Florida, USA

ABSTRACT **APETx3, a novel peptide isolated from the sea anemone *Anthopleura elegantissima*, is a naturally occurring mutant from APETx1, only differing by a Thr to Pro substitution at position 3. APETx1 is believed to be a selective modulator of human ether-á-go-go related gene (hERG) potassium channels with a $K_d$ of 34 nM. In this study, APETx1, 2, and 3 have been subjected to an electrophysiological screening on a wide range of 24 ion channels expressed in *Xenopus laevis* oocytes: 10 cloned voltage-gated sodium channels ($Na_V$ 1.2–$Na_V$1.8, the insect channels Dm$Na_V$1, Bg$Na_V$1–1a, and the arachnid channel Vd$Na_V$1) and 14 cloned voltage-gated potassium channels ($K_V$1.1–$K_V$1.6, $K_V$2.1, $K_V$3.1, $K_V$4.2, $K_V$4.3, $K_V$7.2, $K_V$7.4, hERG, and the insect channel *Shaker* IR). Surprisingly, the Thr3Pro substitution results in a complete abolishment of APETx3 modulation on hERG channels and provides this toxin the ability to become a potent ($EC_{50}$ 276 nM) modulator of voltage-gated sodium channels ($Na_V$s) because it slows down the inactivation of mammalian and insect $Na_V$ channels. Our study also shows that the homologous toxins APETx1 and APETx2 display promiscuous properties since they are also capable of recognizing $Na_V$ channels with $IC_{50}$ values of 31 nM and 114 nM, respectively, causing an inhibition of the sodium conductance without affecting the inactivation. Our results provide new insights in key residues that allow these sea anemone toxins to recognize distinct ion channels with similar potency but with different modulatory effects. Furthermore, we describe for the first time the target promiscuity of a family of sea anemone toxins thus far believed to be highly selective.—Peigneur, S., Béress, L., Möller, C., Marí, F., Forssmann, W.-G., Tytgat, J. A natural point mutation changes both target selectivity and mechanism of action of sea anemone toxins. *FASEB J.* 26, 5141–5151 (2012). www.fasebj.org**

*Key Words: voltage-gated sodium channel · voltage-gated potassium channel · ion channel inhibitor · ion channel modulator*

VOLTAGE-GATED SODIUM CHANNELS ($Na_V$ channels) are transmembrane protein complexes that are constituted of an α-subunit of ~260 kDa and up to 4 auxiliary β-subunits (β1–4) of 30–40 kDa. The pore-forming α-subunit alone is sufficient to obtain sodium current; however, coexpression of β-subunits modifies expression level, kinetics, and voltage dependence of channel gating (1). The α-subunit is organized in 4 homologous domains (DI–IV). Each domain consists of 6 putative transmembrane segments (S1–S6) connected by extracellular or intracellular loops. The S4 segments are the most conserved segments, and they contain a basic residue, either Lys or Arg, in every third position. These positively charged S4 segments are believed to function as voltage sensors. They transport gating charges by moving outward on membrane depolarization, thus initiating the voltage-dependent activation, which results in the opening of the channel. The selectivity filter and pore are formed by the transmembrane segments S5 and S6 along with the reentrant segments that are part of the loop that connects the S5 and S6 of each domain. The short intracellular linker that connects the DIII and DIV contains a highly conserved sequence of 3 hydrophobic residues (Ile, Phe, and Met) or IFM motif. Sodium channel inactivation is mediated by this hydrophobic motif, since it serves as an inactivation gate crucial for causing fast inactivation by binding to a receptor. This inactivation gate receptor is located near or within the intracellular mouth of the sodium channel pore.

Sea anemones have become "medicinal chemists" of unprecedented skills by evolving a unique peptide

Abbreviations: APETx, *Anthopleura elegantissima* toxin; ASIC, acid-sensing ion channel; hERG, human ether-á-go-go related gene; HWTX, huwentoxin; $K_V$ channel, voltage-gated potassium channel; $Na_V$ channel, voltage-gated sodium channel; RP-HPLC, reverse-phase high-performance liquid chromatography; TTX, tetrodotoxin

[1] Correspondence: Laboratory of Toxicology, University of Leuven (KU Leuven), Campus Gasthuisberg O&N2, Herestraat 49, PO Box 922, 3000 Leuven, Belgium. E-mail: jan.tytgat@pharm.kuleuven.be

doi: 10.1096/fj.12-218479

This article includes supplemental data. Please visit *http://www.fasebj.org* to obtain this information.

biochemistry and neuropharmacology to develop components that ensure complete shutdown of the nervous system of their prey. Although a number of sea anemone toxins have been isolated and characterized, these animals remain understudied in comparison with other venomous animals, such as scorpions, spiders, cone snails, and snakes. Sea anemones are a known pharmacological treasure of biological active compounds acting on a diverse panel of ion channels, such as $Na_V$ and voltage-gated potassium ($K_V$) channels, TRPV1 channels, or acid-sensing ion channels (ASICs) (2–4). Out of this group, toxins that target sodium channels are the best studied so far, with >100 known toxins (5). Sea anemone sodium channel toxins can be divided into 3 structural classes, based on their structural differences and activity profile (4, 6–8). All toxins belonging to these three classes exert the same pharmacological activity. They are believed to bind to the channel at receptor site 3. On binding at site 3, these toxins trap the voltage-sensing segment S4 of DIV in its inward position: this prevents the normal outward movement of the voltage sensors and herewith the conformational changes necessary for fast inactivation (9).

To date, 7 toxins from *Anthopleura elegantissima* have been isolated and characterized: APE1-1, APE1-2, APE2-2, and ApC, which are type 1 sodium channel toxins; and APETx1, a modifier of the human ether a go-go related gene (hERG) $K^+$ channel; APETx2, which specifically inhibits ASIC3; and APEKTx1, a potent and selective $K_V1.1$ inhibitor (8, 10–13). APETx1 has been well characterized, and it was first reported to be a selective modulator of hERG channels with an $EC_{50}$ value of 34 nM, although it also exerts some activity over other $K_V$ channels at higher concentrations (Supplemental Fig. S1 and ref. 10). It is thought that APETx1 binds to the outer vestibule of the hERG channel. Toxin binding causes a shift in the voltage dependence of both activation and inactivation curves, resulting in a blockage of the potassium current. Note that full inhibition is not observed, even at high concentrations. Its interaction with hERG channels is voltage dependent, and it suggests that APETx1 exerts a preferential affinity for the closed state of the channel (10, 14). Further structure-function studies have highlighted amino acids on the hERG channel, which are key residues for APETx1 interaction (15).

APETx2 was found to be a potent and selective inhibitor of ASIC3 channels. The current through these ASIC3 channels is reversibly inhibited by APETx2 with an $IC_{50}$ value of 63 nM (8). ASIC3 channels are mainly expressed in sensory neurons and have been identified to play an important role in acid-induced hyperalgesia and in high-intensity pain stimuli (8, 16–18). As such, APETx2 has been a valuable tool to study these channels. *In vivo* studies have shown that administration of APETx2 prevents postoperative acid-induced inflammatory pain (19), (20). Recently, it was found that APETx2 could substantially inhibit tetrodotoxin (TTX)-resistant currents and to a lesser extend TTX-sensitive currents in rat DRG neurons. It was shown that the observed inhibition of $Na_V1.8$ channels resulted from a rightward shift in the voltage dependence of activation and a reduction in the maximal macroscopic conductance (21). Similar to ASIC3 channels, $Na_V1.8$ channels are also expressed in sensory neurons, and they are involved in inflammatory pain. $Na_V1.8$ inhibitors can produce analgesic effects *in vivo* (22–24). The knowledge that APETx2 can exhibit target promiscuity indicates that part of the observed analgesic effect of APETx2 *in vivo* may result from an inhibition of the $Na_V1.8$ conductance (21).

Since these experiments were done in DRG neurons, little information on the $Na_V$ subtype- or phyla-selectivity is available for APETx2.

Here we present the biochemical analysis and electrophysiological characterization of APETx3, a natural occurring mutant of APETx1 differing by a Thr to Pro substitution at position 3. APETx3 is a novel sodium channel toxin, structurally unrelated to the existing classes of sea anemone toxins targeting sodium channels. Furthermore, we re-evaluated the selectivity of APETx1 and APETx2 to show that they are not as selective as previously thought.

## MATERIALS AND METHODS

### Purification and toxin identification

The toxin APETx3 was isolated as described previously (10, 13). The fraction containing APETx3 was further purified by reverse-phase high-performance liquid chromatography (RP-HPLC) with a semipreparative Vydac C18 column (4.6×250 mm; Grace, Columbia, MD, USA). Solvent A was 0.1% TFA in water, and solvent B was 0.085% TFA in acetonitrile. A linear gradient from 0 to 80% solution B was carried out for 80 min at a flow rate of 1 ml/min. A second purification was performed with the same column using a linear gradient from 20 to 40% solution B at a flow rate of 0.2 ml/min. All fractions were dried by speed-vac evaporation and stored at −20°C.

APETx1 was purified as previously described (10). Synthetic APETx2 and huwentoxin (HWTX) IV were purchased from Smartox Biotechnology (Grenoble, France). The purity of these toxins was examined using RP-HPLC as described above.

### Biochemical characterization of toxins

The mass of APETx1 and APETx2 was verified by ESI-MS using a LCQ Deca XP spectrometer (Thermo Finnigan, Waltham, MA USA).

### Sequence determination

The amino acid sequences of APETx1 and APETx2 were verified by Edman degradation using an automated Protein Sequencer PPSQ-33A (Shimadzu, Kyoto, Japan).

For APETx3, the peptide was reduced and alkylated as described previously and adsorbed onto Biobrene-treated fiberglass filter. Amino acid sequencing was carried out by Edman degradation using a Procise model 491A sequencer (Applied Biosystems, Foster City, CA, USA). The concentration of the peptide was determined by using the calibrated

absorbencies of the first 3 PTH-amino acid residues on samples that were not reduced and alkylated.

### Expression of voltage-gated ion channels in *Xenopus laevis* oocytes

For the expression of $Na_V$ channels (r$Na_V$1.2, r$Na_V$1.3, r$Na_V$1.4, h$Na_V$1.5, m$Na_V$1.6, r$Na_V$1.7, r$Na_V$1.8; the insect channels Dm$Na_V$1 and Bg$Na_V$1; the arachnid channel Vd-$Na_V$1; and the auxiliary subunits rβ1, hβ1, and TipE) and of $K_V$ channels ($K_V$1.1-$K_V$1.6, $K_V$2.1, $K_V$3.1, $K_V$4.2, $K_V$4.3, $K_V$7.2, $K_V$7.4, hERG, and the insect channel *Shaker* IR) in *Xenopus* oocytes, the linearized plasmids were transcribed using the T7 or SP6 mMessage-mMachine transcription kit (Ambion, Carlsbad, CA, USA). The harvesting of stage V–VI oocytes from anesthetized female *X. laevis* frogs was previously described (25). Oocytes were injected with 50 nl of cRNA at a concentration of 1 ng/nl using a microinjector (Drummond Scientific, Broomall, PA, USA). The oocytes were incubated in a solution containing 96 mM NaCl, 2 mM KCl, 1.8 mM $CaCl_2$, 2 mM $MgCl_2$, and 5 mM HEPES (pH 7.4), supplemented with 50 μg/ml gentamicin sulfate.

### Electrophysiological recordings

Two-electrode voltage-clamp recordings were performed at room temperature (18–22°C) using a Geneclamp 500 amplifier (Molecular Devices, Downingtown, PA, USA) controlled by a pClamp data acquisition system (Axon Instruments, Union City, CA, USA). Whole-cell currents from oocytes were recorded 1-4 days after injection. Bath solution composition was the following (in mM): 96 NaCl, 2 KCl, 1.8 $CaCl_2$, 2 $MgCl_2$, and 5 HEPES (pH 7.4). Voltage and current electrodes were filled with 3 M KCl. Resistances of both electrodes were kept between 0.5 and 1.5 MΩ. The elicited currents were filtered at 1 kHz and sampled at 20 kHz using a 4-pole low-pass Bessel filter. Leak subtraction was performed using a −P/4 protocol. To avoid overestimation of a potential toxin-induced shift in the current-voltage relationships of inadequate voltage control when measuring large sodium currents in oocytes, only data obtained from cells exhibiting currents with peak amplitude $< 2$ μA were considered for analysis. For the electrophysiological analysis of toxins, a number of protocols were applied from a holding potential of −90 mV with a start-to-start interval of 0.2 Hz. Sodium current traces were evoked by 100-ms depolarizations to $V_{max}$ (the voltage corresponding to maximal sodium current in control conditions). The current-voltage relationships were determined by 50-ms step depolarizations between −90 and 70 mV, using 5-mV increments. The sodium conductance ($g_{Na}$) was calculated from the currents according to Ohm's law: $g_{Na} = I_{Na}/(V - V_{rev})$, where $I_{Na}$ represents the $Na^+$ current peak amplitude at a given test potential $V$, and $V_{rev}$ is the reversal potential. The values of $g_{Na}$ were plotted as a function of voltage and fitted using the Boltzmann equation: $g_{Na}/g_{max} = \{1 + [\exp(V_g - V)/k]\}^{-1}$, where $g_{max}$ represents maximal $g_{Na}$, $V_g$ is the voltage corresponding to half-maximal conductance, and $k$ is the slope factor. Toxin-induced effects on the steady-state inactivation were investigated using a standard 2-step protocol. In this protocol, 100-ms conditioning 5-mV step prepulses ranging from −90 to 70 mV were followed by a 50-ms test pulse to −30 or −10 mV. Data were normalized to the maximal $Na^+$ current amplitude, plotted against prepulse potential and fitted using the Boltzmann equation: $I_{Na}/I_{max} = ((1 - C)/\{1 + \exp[(V - V_h)/k]\}) + C$, where $I_{max}$ is the maximal $I_{Na}$, $V_h$ is the voltage corresponding to half-maximal inactivation, $V$ is the test voltage, $k$ is the slope factor, and $C$ is a constant representing a noninactivating persistent fraction (close to 0 in control). The recovery from inactivation was assayed with a double-pulse protocol, where a 100-ms conditioning pulse to −30 or −10 mV was followed by a 50-ms test pulse to the same voltage. Both pulses were interspersed by a repolarization to −90 mV for a gradually increasing time interval (1-40 ms). The $I_{Na}$ obtained in the test pulse was normalized to the $I_{Na}$ obtained in the conditioning pulse, plotted against the corresponding time interval, and fitted with the following exponential equation: $f(t) = Ae^{-t/\tau} + C$, where $t$ is time, $A$ is the amplitude of the current, τ is the time constant for the fast inactivation, and $C$ is a constant representing a noninactivating persistent fraction (close to 0 in control).

To assess the concentration-response relationships, data were fitted with the Hill equation: $y = 100/[1 + (EC_{50}/[\text{toxin}])^h]$, where $y$ is the amplitude of the toxin-induced effect, $EC_{50}$ is the toxin concentration at half maximal efficacy, [toxin] is the toxin concentration, and $h$ is the Hill coefficient. The time constants τ of the $Na_V$ channel fast inactivation were measured directly from the decay phase of the recorded $Na^+$ current using a single exponential fit. Comparison of 2 sample means was made using a paired Student's $t$ test ($P<0.05$). All data are presented as means ± SE of ≥5 independent experiments ($n \geq 5$). All data were analyzed using pClamp Clampfit 10.0 (Molecular Devices) and Origin 7.5 software (Originlab, Northampton, MA, USA).

## RESULTS

### Purification and toxin identification

The screening of fractions obtained from the sea anemone *A. elegantissima*, after anion and cation exchange and gel filtration, yielded one fraction, APETx3, that was active on $Na_V$ channels. This fraction was further purified in 2 steps using RP-HPLC.

### Biochemical characterization

With ESI-MS analysis, a mass of 4544.7 Da APETx3 was observed. The theoretical mass of 4545.0 Da corresponds well with the experimentally determined mass. The intact toxin was subjected to Edman degradation. The following sequence was obtained: GTPCYCGKTIGIYWFGTKTCPSNRGYTGSCGYFLGICCYPVD (**Fig. 1**).

The molecular mass and primary sequence of APETx1 and APETx2 were determined to verify the purity of both toxins. Both the mass spectrum analysis and amino acid sequence determination were in complete accord with previous reports (8, 10).


**Figure 1.** Amino acid sequence of APETx3 and alignment with APETx1 and APETx2. Amino acid residues identical with APETx3 are shown on gray background, cysteine residues are in red.

The sequence data of APETx3 were deposited in the UniProt Knowledgebase under accession number B3EWF9.

## Electrophysiological recordings

### *APETx3 is a modulator of $Na_V$ channels*

APETx3 was screened against a panel of 7 mammalian $Na_V$ channel isoforms and 3 insect $Na_V$ isoforms (**Fig. 2**). Among the mammalian isoforms, 1 μM APETx3 slowed the inactivation of $Na_V1.2$, $Na_V1.3$, $Na_V1.4$, and $Na_V1.6$. $Na_V1.7$ and the TTX-resistant channels $Na_V1.5$ and $Na_V1.8$ were not affected by APETx3. Furthermore, the same concentration of toxin had a profound effect on the inactivation of the insect isoforms $DmNa_V1$ and $BgNa_V1$. APETx3 completely inhibited their inactivation, resulting in sustained noninactivating currents. Although APETx3 could also slow down its inactivation, the arachnid channel $VdNa_V1$ was less sensitive compared with the other insect $Na_V$ channel isoforms. Concentration-response curves were constructed for $Na_V1.6$ and $DmNa_V1$. $EC_{50}$ values yielded 2265 ± 185 and 276 ± 37 nM, respectively (Fig. 2*B*). The most toxin-sensitive isoform among the mammalian $Na_V$ channels, $Na_V1.6$, and the insect $Na_V$ channel $DmNa_V1$ were used to further investigate the characteristics of APETx3 in inducing modulation of channel gating (**Fig. 3*A, B***). No shift in the midpoint of activation was observed (Supplemental Table S1). However, 1 μM APETx3 could significantly shift the voltage dependence of steady-state inactivation. The $V_{1/2}$ shifted from −69 ± 0.3 to −62 ± 0.2 mV for $Na_V1.6$ ($n$=4; $P$<0.05). For $DmNa_V1$ channels, the $V_{1/2}$ shifted from −51 ± 0.2 to −43 ± 0.4 mV ($n$=6; $P$<0.05). From Fig. 3*A, B*, it can be seen that the steady-state inactivation became incomplete after toxin addition. For $Na_V1.6$, a 56 ± 2% noninactivating current component was observed, while for $DmNa_V1$, a complete removal of steady-state inactivation can be seen.

To verify that APETx3 does bind to neurotoxin site 3, competitive binding experiments were performed using CgNa, a type I sea anemone toxin known to bind to site 3 of $Na_V$ channels. Application of CgNa at its $EC_{50}$ value of 250 nM (26) resulted in an 18 ± 3% noninactivating current component of $Na_V1.6$ channels. Subsequent addition of $EC_{50}$ concentrations of APETx3 did not result in further slowing down of inactivation (Fig. 3*C*).

### *APETx3 is not a modulator of hERG channels*

APETx3 can be considered as a natural mutant of APETx1, as they only differ in one residue (Fig. 1). Therefore, we decided to investigate whether APETx3 displays the same activity profile of APETx1. APETx1 has been reported to be a selective and potent modulator of hERG channels with an $EC_{50}$ value of 34 nM (8), a result that we have been able to confirm (**Fig. 4**). Interestingly, even at concentrations up to 50 μM, APETx3 failed to induce any modulation of hERG channels (Fig. 4).

Since it has been reported that APETx1 exhibits activity for other $K_V$s, although only in higher concentrations (8), we tested the activity of APETx3 against 13

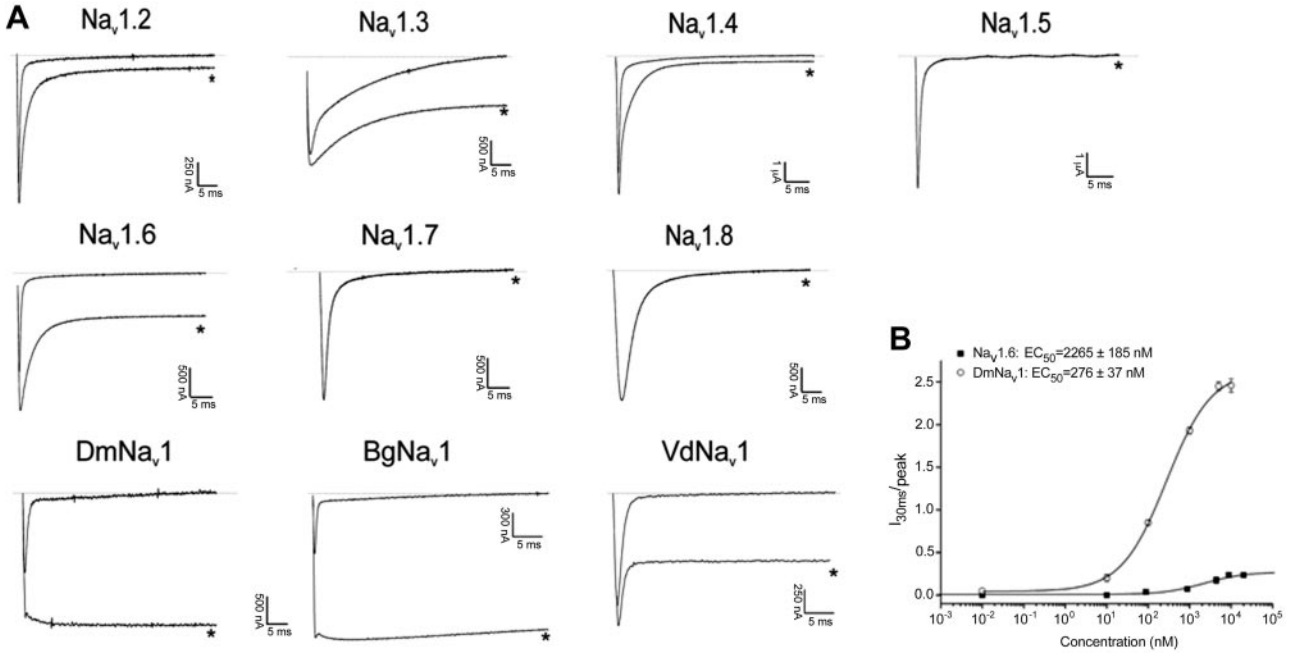


**Figure 2.** Electrophysiological characterization of APETx3 on $Na_V$ channels. *A*) Activity profile of APETx3 on several $Na_V$ channel isoforms. Representative whole-cell current traces in control and toxin conditions are shown. Dotted line indicates 0 current level; asterisk indicates steady-state current trace after application of 1 μM toxin. Traces represent ≥3 independent experiments ($n$≥3). *B*) Concentration-response curves for $Na_V1.6$ and $DmNa_V1$, indicating the concentration dependence of the APETx3-induced increase of the $Na^+$ peak current.

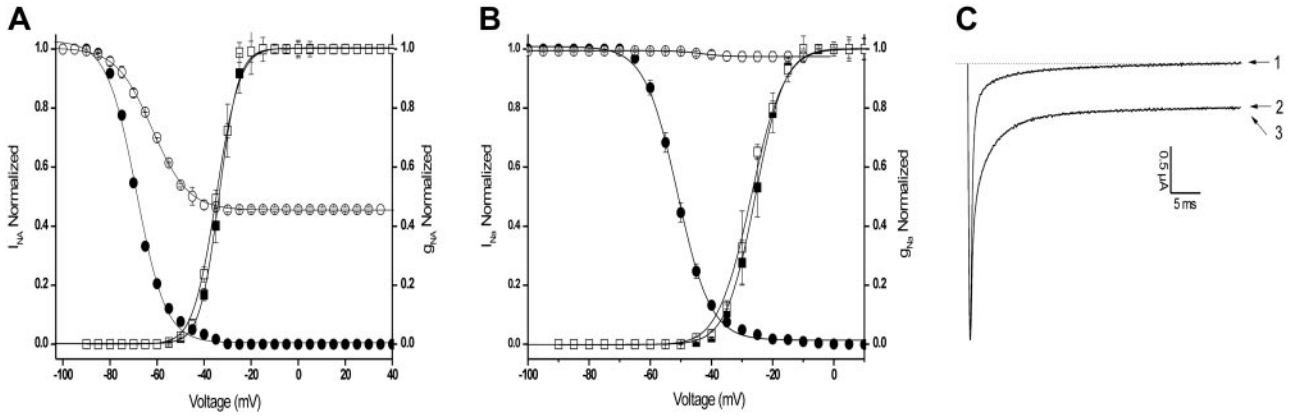


**Figure 3.** *A*, *B*) Electrophysiological characterization of APETx3 on $Na_V1.6$ (*A*) and $DmNa_V1$ (*B*) channels. Steady-state activation and inactivation curves in control conditions (solid symbols) and toxin conditions (1 μM APETx3; open symbols). *C*) Competitive experiment to indicate that APETx3 does bind at site 3. Representative traces are shown: *1*) control; *2*); after application of 250 nM CgNa (26); and *3*) after subsequent addition of 2200 nM APETx3.

different $K_V$ channel isoforms. APETx3 showed no activity against members of the *Shaker* ($K_V1.1$–$K_V1.6$ and the insect channel *Shaker* IR), *Shab* ($K_V2.1$), *Shaw* ($K_V3.1$), *Shal* ($K_V4.2$ and $K_V4.3$) subfamilies, nor did APETx3 exhibit affinity for KCNQ gene family encoded $K_V$ channels, such as $K_V7.2$ and $K_V7.4$ (Supplemental Fig. S1).

*APETx1 inhibits the conductance through $Na_V$ channels*

At a concentration of 1 μM, APETx1 was tested for its activity against the same panel of $Na_V$ channel isoforms. Remarkably, it was found that APETx1 could inhibit the sodium conductance of all mammalian $Na_V$ channel isoforms tested except $Na_V1.7$ (**Fig. 5*A***). APETx1 showed the highest affinity for $Na_V1.8$, as the sodium peak amplitude ($I_{Na}$) was reduced by 89 ± 2% ($n$=4; $P$<0.05). $Na_V1.2$ and $Na_V1.6$ were equally sensitive for this toxin since 1 μM APETx1 inhibited the peak amplitude by 61 ± 4 and 59 ± 1% ($n$=3; $P$<0.05), respectively. The same concentration of toxin could inhibit $Na_V1.4$ and $Na_V1.5$ by 56 ± 2 and 50 ± 2% ($n$=3; $P$<0.5), respectively. $Na_V1.3$ was the less affected by APETx1 since only 5 ± 1% ($n$=3; $P$<0.5) inhibition could be observed. None of the insect $Na_V$ channel isoforms tested were affected by APETx1. To investigate the concentration-response relationships, $EC_{50}$ values were defined for $Na_V1.2$ and $Na_V1.8$ channels. $EC_{50}$ values yielded 31 ± 6 and 92 ± 4 nM, respectively (Fig. 5*B*).

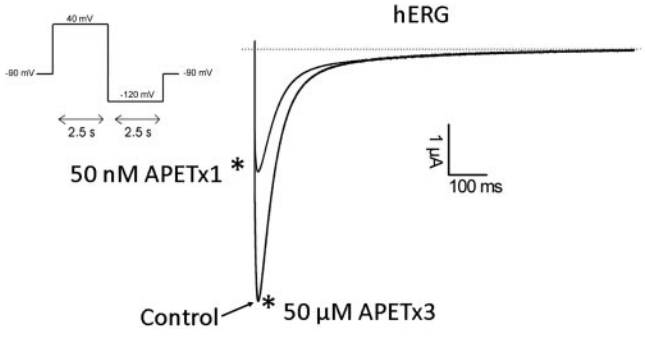


**Figure 4.** Activity of APETx1 and APETx3 on the hERG expressed in *X. laevis* oocytes. Dotted line indicates 0 current level; asterisk indicates steady-state current trace after application of 1 μM toxin.

$Na_V1.2$ channels were used to determine whether APETx1 acts as a pore blocker by physically obstructing the ion pathway or rather as a modulator of channel gating. No shift in the voltage dependence of activation or a significant alteration of the steady-state inactivation curves was observed (Supplemental Fig. S2*A* and Supplemental Table S1). The toxin-induced reduction of peak amplitude was not associated with a shift in the reversal potential, indicating no modification in the ion selectivity after toxin application (Supplemental Fig. S2*B*). APETx1 did not influence the rate of recovery from inactivation (Supplemental Table S1). The time constant of recovery yielded 3 ± 0.04 ms in control conditions and 3 ± 0.1 ms after application of 50 nM APETx1 ($n$=4; $P$<0.05; Supplemental Fig. S2*C*). Furthermore, it should be noted that, even after the application of toxin concentrations up to 20 μM, a residual current of 5-10% remained. For $Na_V1.2$ channels, time value of APETx1 binding yielded 29 ± 3 s ($\tau_{on}$) while unbinding on washout occurred with a time constant of 18 ± 2 s ($\tau_{off}$) (Supplemental Fig. S2*D*).

*APETx2 inhibits the conductance through $Na_V$ channels*

As APETx1 and APETx2 have 64% sequence identity, we examined whether APETx2 also could exert promiscuous activity. This screening revealed that APETx2 exhibits also activity on $Na_V$ channels. However, at a concentration of 1 μM, APETx2 seems to be more active toward $Na_V1.2$, $Na_V1.6$, and $Na_V1.8$ (**Fig. 6*A***). The $I_{Na}$ through $Na_V1.2$ channels was reduced by 57 ± 3% ($n$=5; $P$<0.05), while the same concentration of toxin inhibited the conductance of $Na_V1.6$ channels by 17 ± 2% ($n$=4; $P$<0.05) and $Na_V1.8$ channels by 68 ± 2% ($n$=6; $P$<0.05), respectively. A slowing of inactiva-

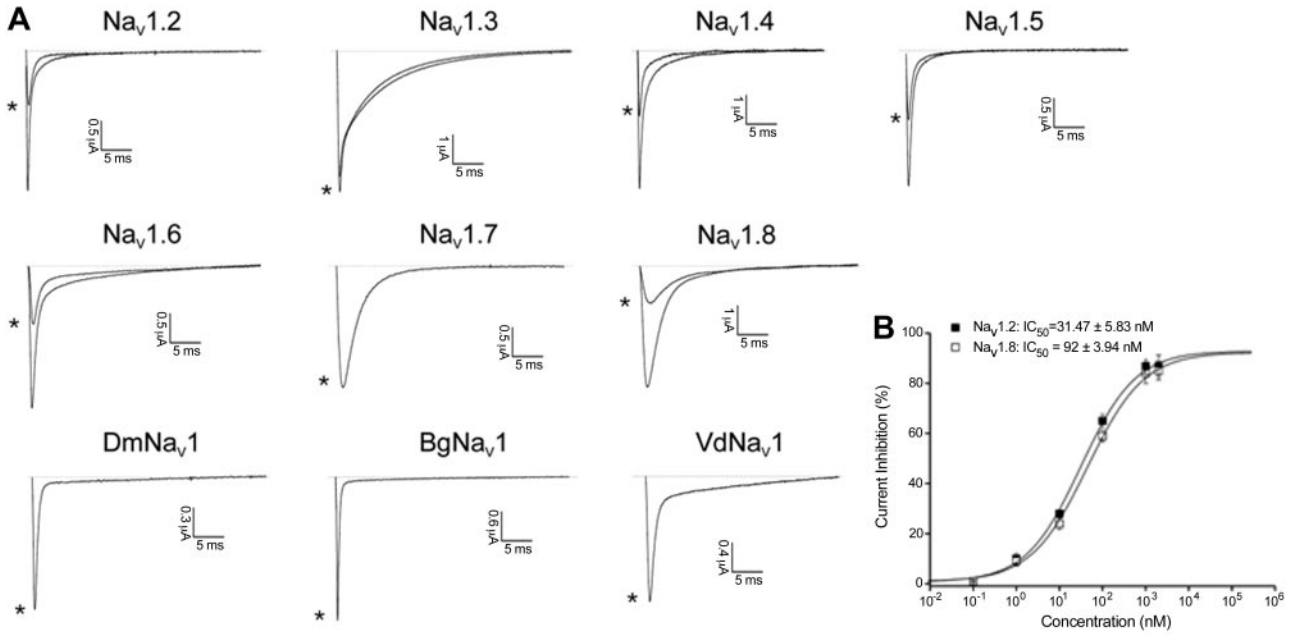


**Figure 5.** Electrophysiological characterization of APETx1 on $Na_V$ channels. *A*) Activity profile of APETx1 on several $Na_V$ channel isoforms. Representative whole-cell current traces in control and toxin conditions are shown. Dotted line indicates 0 current level; asterisk indicates steady-state current trace after application of 1 μM toxin. *B*) Concentration-response curves for $Na_V1.2$ and $Na_V1.8$, indicating the concentration dependence of the APETx1-induced decrease of the $Na^+$ peak current.

tion in real time was observed for $Na_V1.8$ channels. The concentration-response curves were constructed, and $EC_{50}$ values yielded 114 ± 25 and 55 ± 10 nM for $Na_V1.2$ and $Na_V1.8$ channels, respectively (Fig. 6*B*).

Similar to APETx1, APETx2 did not alter the voltage dependence of activation or steady-state inactivation (Supplemental Fig. S3*A* and Supplemental Table S1). Toxin application did not influence the current-voltage relationship or the ion selectivity (Supplemental Fig. S3*B*). The rate of recovery from inactivation was not different from control conditions (Supplemental Fig. S3*C* and Supplemental Table S1). APETx2 inhibited $Na_V1.2$ channels with a $\tau_{on}$ of 31 ± 4 s, and inhibition was reversible on washout ($\tau_{off}$=8±2 s; Supplemental Fig. S3*D*).

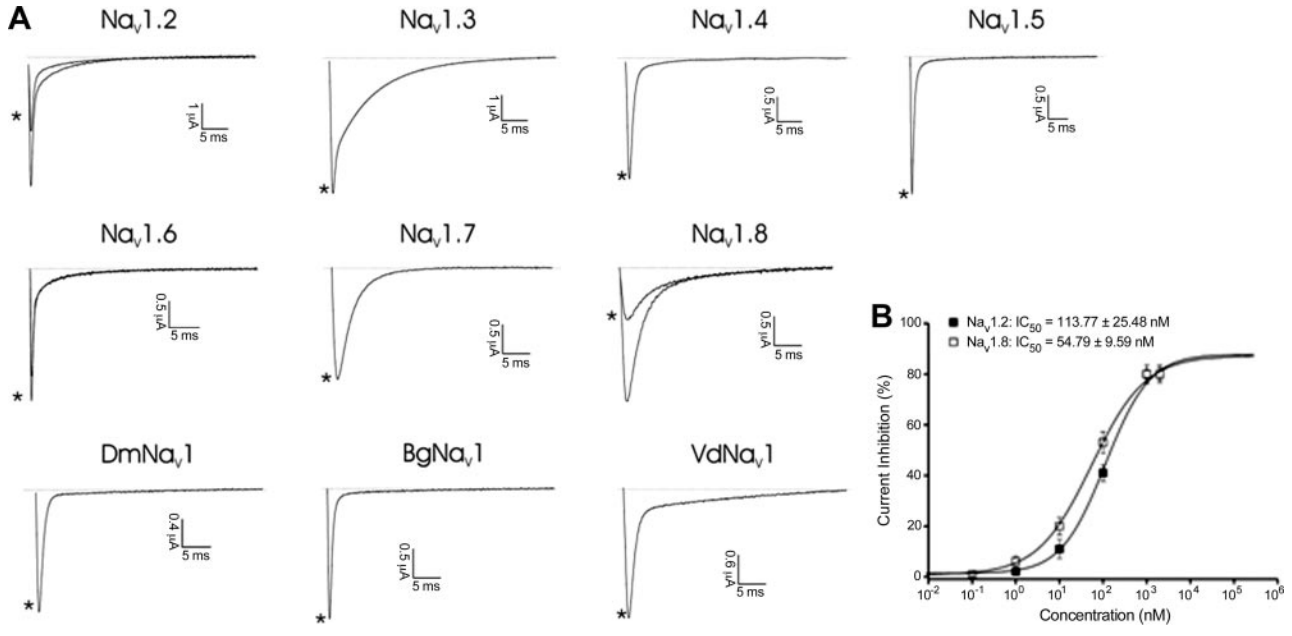


**Figure 6.** Electrophysiological characterization of APETx2 on $Na_V$ channels. *A*) Activity profile of APETx2 on several $Na_V$ channel isoforms. Representative whole-cell current traces in control and toxin conditions are shown. Dotted line indicates 0 current level; asterisk indicates steady-state current trace after application of 1 μM toxin. *B*) Concentration-response curves for $Na_V1.2$ and $Na_V1.8$, indicating the concentration dependence of the APETx2-induced decrease of the $Na^+$ peak current.

*Are APETx1 and APETx2 modulators of gating kinetics or pore blockers?*

To investigate whether the inhibition of the sodium conductance depends on toxin interaction with the inactivated state of the α-subunit, the activity of APETx1 and APETx2 was tested on $Na_V1.2$ channels in which the fast inactivation has been removed (27). Removal of fast inactivation is obtained by mutating the highly conserved hydrophobic residues that contribute to the inactivation gate of $Na_V$ channels (26). Fast inactivation-deficient $Na_V1.2$ channels have the Ile1488, Phe1489, and Met1490 residues replaced by Gln residues ($Na_V1.2$ IFM/QQQ channels). A concentration of 1 μM APETx1 could reduced the $I_{Na}$ by 59 ± 3% ($n$=6; $P$<0.05), while the same concentration of APETx2 inhibited the current through the $Na_V1.2$ IFM/QQQ channels by 22 ± 3% ($n$=4; $P$<0.05; **Fig. 7**). For both toxins, a shift in the time to peak ($T_{peak\ Na}$) could be on their application. Addition of APETx1 shifted the $T_{peak\ Na}$ from 0.4 ms in control conditions to 2 ms ($n$=6; $P$<0.01); 1 μM APETx2 caused a more modest but still significant shift from 0.3 to 0.7 ms ($n$=4; $P$<0.01). For comparison purposes, identical experiments were done using 50 and 100 nM of TTX; no shift in $T_{peak\ Na}$ was noticed ($n$=3; $P$<0.01).

To determine whether inhibition occurs during the closed or open state of the channel, 1 μM toxin was applied to the bath solution with oocytes clamped at −90 mV, allowing interaction with the membrane for 2 min without depolarizing the membrane. After 2 min, currents were elicited by a depolarizing pulse to 0 mV. The obtained currents in presence of toxin were normalized to the currents obtained in the same cells in control conditions. No inhibition was observed when APETx1 or APETx2 was applied to the oocytes without applying depolarizing pulses (**Fig. 8*A***). This indicates that there is no toxin interaction with the channel in the closed state and suggests that membrane depolarization and hence most likely also channel opening is required to allow the toxin to bind.

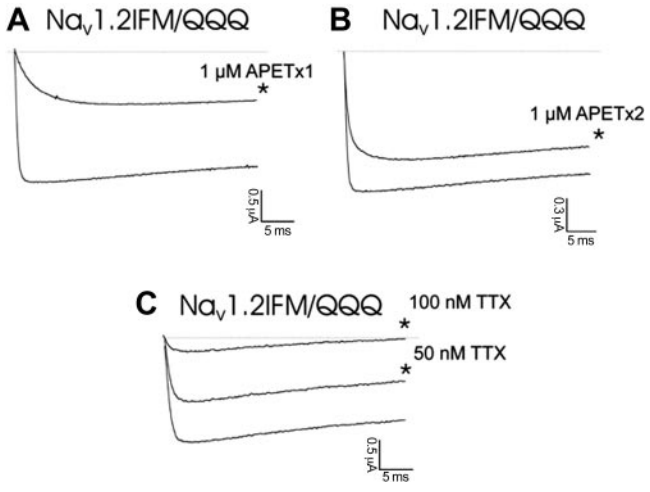


**Figure 7.** *A*, *B*) Effect of APETx1 (*A*) and APETx2 (*B*) on fast inactivation-deficient $Na_V1.2$ channels. *C*) Effects of 50 and 100 nM TTX, shown for comparison. Dotted line indicates 0 current level; asterisk indicates steady-state current trace after application of 1 μM toxin.

To investigate whether inhibition was use dependent, oocytes expressing $Na_V1.2$ were submitted to depolarizing pulses at differing frequencies, both in control conditions and after application of 1 μM toxin (Fig. 8*B*). No difference in the degree of inhibition was observed at differing frequencies, suggesting that the toxin-induced inhibition is not use dependent.

To determine a possible binding site of APETx1 and APETx2, we investigated whether both toxins share a binding site with HWTX IV, a tarantula toxin that exerts the same characteristics of channel modulation and the binding site of which has been studied in depth (28). Application of HWTX IV at its $EC_{50}$ concentration of 55 nM reduced the sodium conductance of $Na_V1.2$ channels by 48 ± 2% (experimentally determined by constructing a concentration-response curve with for each point $n$≥3). Interestingly, subsequent addition of $EC_{50}$ concentrations of APETx1 or APETx2 resulted in further reduction of the sodium conductance (Fig. 8*C*). However, the observed reduction was, for both APETx1 and APETx2, <50% of the remaining current. Subsequent addition of $EC_{50}$ concentrations of APETx1 inhibited the remaining $Na_V$ channels by 43 ± 2% ($n$=4) while for APETx2, an inhibition of 37 ± 1% ($n$=3) was observed after preceding HWTX IV application (Fig. 8*D*). Since APETx1 and APETx2 failed to compete for the HWTX IV binding site, we next investigated whether both toxins interact with neurotoxin receptor site 1. TTX, a well-known pore blocker of $Na_V$ channels (29), was used for competitive binding experiments (Fig. 8*E*). Application of TTX at its $IC_{50}$ value resulted in a blockage of half the expressed $Na_V1.2$ channels, as a 50% decrease of the sodium current peak amplitude was observed. Subsequent and additional application of the $EC_{50}$ value of APETx1 or APETx2 did not result in an additional reduction of the peak amplitude. Similar experiments were conducted using the μ-conotoxin KIIIA. This short peptide, isolated from *Conus kinoshitai*, is known to bind a microsite within the pore different from the TTX binding site 1 (30, 31). Application of KIIIA at its $IC_{50}$ concentration of 60 nM (30) halved the sodium conductance of $Na_V1.2$ channels. Subsequently, addition of $EC_{50}$ concentrations of APETx1 or APETx2 failed to introduce any further reduction of the sodium conductance (Fig. 8*E*). These results suggest that both APETx1 and APETx2 do interact with neurotoxin binding site 1.

## DISCUSSION

### APETx3

Sea anemone venom is a known source of unique peptide toxins, which can be used as invaluable tools for studying structure and function of ion channels and receptors. Here we report the characterization of a

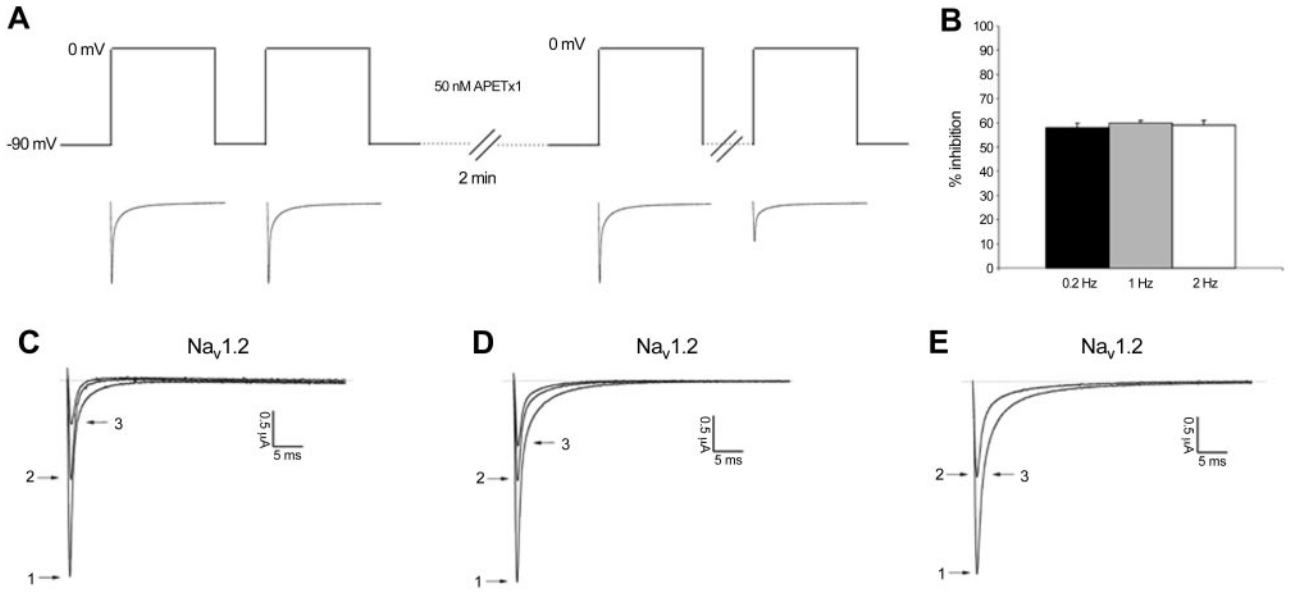


**Figure 8.** Electrophysiological determination of possible binding sites. *A*) To investigate the state dependence of inhibition. the following protocol was used. As control, a series of depolarizing pulses was applied to an oocyte expressing NaV1.2 channels. Thereafter, 30 nM APETx1 was added, and no pulsing was performed for 2 min. Next, a similar series of pulses was executed. No inhibition was observed after the 2-min incubation. Inhibition only occurred after membrane depolarization. *B*) Possible use dependence of toxin inhibition was studied by applying 50 nM APETx1 to oocytes subjected to depolarizing pulses at different frequencies. *C*) Competitive experiment to indicate that APETx1 does not compete with HWTX IV. Representative traces are shown: *1*) control; *2*) after application of 55 nM HWTX IV (46); and *3*) after subsequent addition of 30 nM APETx1 (46). *D*) Competitive experiment to indicate that APETx2 does not compete with HWTX IV. Representative traces are shown: *1*) control; *2*) after application of 55 nM HWTX IV (46); and *3*) after subsequent addition of 115 nM APETx2 (46). *E*) Competitive experiment to indicate that APETx1 or APETx2 does bind at site 1. Representative traces are shown: *1*) control; *2*) after application of 1 nM TTX or 60 nM KIIIA (46); and *3*) after subsequent addition of 30 nM APETx1 or 115 nM APETx2.

novel peptide from the sea anemone *A. elegantissima*, APETx3. This toxin can be seen as a natural occurring mutant from APETx1, only differing in 1 aa at position 3 (Thr3Pro). Remarkably, this point mutation dramatically alters the pharmacology profile of the toxin, with APETx3 being inactive and APETx1 being highly active on hERG channels. Furthermore it allows these toxins to exert a differing pharmacology on the same target, namely $Na_V$ channels: APETx3 slows down the inactivation while APETx1 inhibits the conductance. In other words, the point mutation flips the toxin from an inhibitor to a drug that locks $Na_V$ channels open. The APETx3 induced alteration in steady-state inactivation most likely results from the toxin binding to site 3. Many α-scorpion toxins and sea anemone toxins are known to bind to this site and on binding they trap the voltage-sensing S4 of DIV in its inward or deactivated position, hereby preventing the structural movements required for fast inactivation (32, 33). Several toxins capable of binding site 3 have been isolated from sea anemones. However, APETx3 is unrelated to any of the 3 existing sea anemone classes known to act on $Na_V$ channels and it represents the first member of a fourth class of site 3 binding toxins.

The insect-specificity of APETx3 is demonstrated by the complete inhibition of the inactivation of the insect $Na_V$ channels $DmNa_V1$ and $BgNa_V1.1$, and it is furthermore emphasized by the 10-fold difference in $EC_{50}$ values between mammalian ($Na_V1.6$) and insect ($DmNa_V1$) channels. This preference for insect $Na_V$ channels suggests that APETx3 can be used as an insecticide (34, 35).

The functional differences between APETx1 and APETx3 raise an intriguing structure-function conundrum. APETx1 and APETx3 only differ from each other by a Thr to Pro substitution at position 3. It is well known that prolines can induce a structural kink in a peptide structure. It is possible that the Thr3Pro substitution in APETx3 results in a conformational change that allows APETx3 to expose a contact surface differing from that of APETx1, which might explain the functional differences between these peptides. However, detailed structural studies will are required to verify this hypothesis.

### APETx1

APETx1 and APETx2 are the first sea anemone peptides shown to inhibit the conductance of $Na_V$ channels. Here we show that APETx1 is a promiscuous toxin, capable of inhibiting $Na_V$ channels in the same concentration range as it is active on hERG channels. APETx1 inhibits the mammalian isoforms $Na_V1.2$-$Na_V1.6$ and $Na_V1.8$. Remarkably, no effect was observed on the insect $Na_V$ channel isoforms. Since APETx3 is an insect-specific modulator of $Na_V$, it can be discerned that the point mutation at position 3 influences the phyla-specificity of APETx-like peptides.

Similar to the inhibition of potassium currents though hERG channels, no complete inhibition of the sodium currents could be achieved, even at high concentrations of APETx1. However, there are differences in the current inhibition effected by APETx1 for $Na_V$ and hERG channels. Contrary to what is reported for hERG modulation, no modulation in the voltage dependence of activation or steady-state inactivation was observed. APETx1 does not seem to interact with the closed state of the sodium channel. It was also noted that APETx1 inhibition is not use dependent. Competitive experiments with TTX and the μ-conotoxin KIIIA, two known pore-blocker toxins, led to the assumption that APETx1 does inhibit $Na_V$ channels by binding at site 1 or close by. Furthermore, with the use of fast inactivation-deficient $Na_V1.2$ channels, it was shown that APETx1 does not rely on the inactivated state to exhibit its conductance inhibiting activity. In these experiments, it could be seen that APETx1 causes a significant shift in the time to peak, possibly indicating a modified transition from closed to open state on depolarization.

**APETx2**

With the use of the oocyte expression system, APETx2 was submitted to a screening on several mammalian and insect $Na_V$ channel isoforms. It was found that APETx2 could also inhibit $Na_V1.2$ channels with the same potency as $Na_V1.8$ channels. To a lesser extent, the toxin also inhibited the $Na_V1.6$ channel. Further electrophysiological investigations demonstrated that APETx2 has the mechanism of interaction with the channels as APETx1. APETx2 did not alter the voltage dependence of activation or inactivation nor did it influence the reversal potential or the recovery from inactivation. No usedependency was noted, and APETx2 did not seem to rely on the inactivated state to inhibit currents. Furthermore, APETx2 does compete with TTX and μ-conotoxins for their binding site. However, APETx2 did cause a shift in the time to peak of $Na_V1.2$ IFM/QQQ channels.

Studies of interaction of APETx2 with $Na_V1.8$ channels in DRG neurons indicated that this toxin acts as a modulator rather than a pore blocker (21). This finding was substantiated by the small (±5 mV) but significant shift of the voltage dependence of activation toward more depolarized values. Moreover, the toxin-induced slowing down of fast inactivation but not the steady-state inactivation, together with a slight acceleration of the initial phase of recovery suggests that APETx2 destabilizes the inactivated state. The results obtained for $Na_V1.2$ channels in oocytes are in accord with the results for $Na_V1.8$ channels in DRG neurons, except for the 5-mV shift in activation and the small acceleration in recovery from inactivation. However, since both results were obtained in different expression systems (patch clamp *vs.* voltage clamp), it is possible that these small differences can be explained as such. Since both systems use different cells to express channels, potential differences in post-translational modifications of channels and differences in expression of auxiliary subunits might influence kinetics of channel gating. Furthermore, the need for multiple pharmacological manipulations to isolate a specific channel current in neurons, which are unnecessary in *Xenopus* oocytes, and differences in membrane composition together with inherent differences in osmolarity of the recording solutions can provide an explanation for the differences observed between both expression systems.

For both APETx1 and APETx2, it can be concluded that the exact mechanism of action still needs to be determined. Peptide toxins with the ability to inhibit >1 ion channel or receptor are mostly found in spider venoms, more particular tarantula venoms. For example, Hanatoxin I from the tarantula *Grammostola spatulata*, is a gating modifier of $Ca_V2$ channels as well $K_V2$ and $K_V4$ (36, 37). Another example can be found in toxins isolated from the venom of *Grammostola rosea*, which act as gating modifiers of both $Na_V$ and hERG, but not $K_V1$ channels, by shifting the voltage dependence of activation toward more positive potentials (38). From the Chinese tarantula *Ornithoctonus huwena*, two toxins, HWTX-I and HWTX-IV, have been isolated and characterized in depth (39, 40). Both HWTX-I and HWTX-IV are capable of inhibiting, in nanomolar concentrations, TTX-sensitive $Na_V$ channels (28, 41). Interestingly, similar to APETx1 and APETx2, this inhibition occurs without altering the voltage dependence of activation or inactivation. Using site-directed mutagenesis analysis, it was found that HWTX-IV binds to site 4, which is mainly located at the S3–S4 linker of DII. It is proposed that the voltage sensor of DII is trapped in its inward position as a result of HWTX-IV binding, thereby hampering the sodium conductance (28). Competition experiments show that APETx1 and APETx2 do not compete with the HWTX IV binding site. Promiscuous tarantula toxins adopt the ICK motif and share little to no identity with the APETx-like peptides, which are members of the cysteine-stabilized αβ (Csαβ) structural family. Nevertheless, it is noteworthy that all promiscuous spider toxins known up to date are believed to interact with the voltage-sensing modules of their ion channel targets. Therefore, one can question whether other toxins that overstep the boundaries of targeting a single ion channel, such as APETx1 and APETx2, are not also expected to interact with the voltage sensor. The electrophysiological data available at present for APETx1 and APETx2 do not prove such an interaction. However, it does also not exclude this. Further structure-function analyses involving site-directed mutagenesis studies, docking, and radiolabeled binding experiments are required to elucidate the site of binding of these peptides to gain further understanding of their mechanism of action.

From the *Anemonia viridis* EST dataset, 12 APETx-like peptides could be indentified (42). Recently, using a 454 pyrosequencing approach, it was shown that two other sea anemones, *Stichodactyla helianthus* and *Bunodosoma granulefera*, also express peptides belonging to the APETx family, suggesting that APETx-like peptides

are conserved throughout sea anemone species (43). Interestingly, several APETx-like peptides possess a proline at position 3, similar to APETx3. Moreover, two other members of this family, BDS-I and BDS-II, characterized as $K_V3.4$ blockers, also contain a proline at position 3 (44). Recently, it was shown that BDS-I, similar to APETx3, could slow the inactivation of TTX-sensitive $Na_V$ currents (45). This indicates that the presence of a proline at position 3 is one of the key determinants for $Na_V$ channel inactivation modulation. However, the target promiscuity of APETx-like peptides, as underlined in this work, necessitates functional characterization to identify the different targets of peptides belonging to the APETx family.

APETx1 and APETx2 are two toxins that are synthetically produced, commercially available, and have been used in *in vivo* experiments. We have demonstrated that caution is required in interpretation of these *in vivo* experiments, since APETx1 and APETx2 are not selective modulators of hERG and ASIC3 channels, respectively, as thus far believed. Our data show that these toxins are promiscuous, targeting $Na_V$ channels with an equal potency. Moreover, they are the first $Na_V$ channel inhibitors from sea anemones reported. Overall, the target promiscuity of APETx1 and APETx2 unravels the family of APETx-like peptides as a yet unexplored treasure of promiscuous toxins. APETx1–3 represent valuable probes for further structure-function studies and herby provide new leads in the development of therapeutic agents for channel related diseases. FJ

The authors thank John N. Wood (University College London, London, UK) for sharing $rNa_V1.8$; A. L. Goldin (University of California, Irvine, CA, USA) for sharing $rNa_V1.2$, $rNa_V1.3$, and $mNa_V1.6$; G. Mandel (State University of New York, Stony Brook, NY, USA) for sharing $rNa_V1.4$; R. G. Kallen (Roche Institute of Molecular Biology, Nutley, NJ, USA) for sharing $hNa_V1.5$; S. H. Heinemann (Friedrich-Schiller-Universität Jena, Jena, Germany) for sharing the rat$\beta$1 subunit; S. C. Cannon (University of Texas Southwestern Medical Center, Dallas, TX, USA) for sharing the h$\beta$1 subunit; M. Keating (University of Utah, Salt Lake City, UT, USA) for sharing hERG; and Martin S. Williamson (Rothhamsted Research, Harpenden, UK) for providing the Para and tipE clone. The $Na_V1.7$ clone was kindly provided by Roche (Basel, Switzerland). The authors are grateful to K. Dong (Michigan State University, East Lansing, MI, USA) for sharing $BgNa_V1.1$ and $VdNa_V1$.The authors thank Dr. Piet Herdewyn and Dr. Eveline Lescrinier for help with experiments. The authors are grateful to Dr. Bert Billen for constructive discussions. The authors thank Sarah Debaveye for her work in molecular biology. The authors thank Dr. Sylvie Diochot (Université de Nice-Sophia-Antipolis, Valbonne, France) for sharing APETx1. This work was supported by the following grants: G.0433.12 (Fonds Wetenschappelijk Onderzoek Vlaanderen), Inter-University Attraction Poles (IUAP) Program 7/19 (Belgian State, Belgian Science Policy), and OT/12/081 (Katholieke Universiteit Leuven).

## REFERENCES

1. Yu, F. H., and Catterall, W. A. (2003) Overview of the voltage-gated sodium channel family. *Genome Biol.* **4,** 207
2. Andreev, Y. A., Kozlov, S. A., Koshelev, S. G., Ivanova, E. A., Monastyrnaya, M. M., Kozlovskaya, E. P., and Grishin, E. V. (2008) Analgesic compound from sea anemone *Heteractis crispa* is the first polypeptide inhibitor of vanilloid receptor 1 (TRPV1). *J. Biol. Chem.* **283,** 23914–23921
3. Honma, T., and Shiomi, K. (2006) Peptide toxins in sea anemones: structural and functional aspects. *Mar. Biotechnol. (N.Y.)* **8,** 1–10
4. Castaneda, O., and Harvey, A. L. (2009) Discovery and characterization of cnidarian peptide toxins that affect neuronal potassium ion channels. *Toxicon* **54,** 1119–1124
5. Bosmans, F., and Tytgat, J. (2007) Sea anemone venom as a source of insecticidal peptides acting on voltage-gated $Na^+$ channels. *Toxicon* **49,** 550–560
6. Oliveira, J. S., Zaharenko, A. J., Ferreira, W. A., Jr., Konno, K., Shida, C. S., Richardson, M., Lucio, A. D., Beirao, P. S., and de Freitas, J. C. (2006) BcIV, a new paralyzing peptide obtained from the venom of the sea anemone *Bunodosoma caissarum.* A comparison with the $Na^+$ channel toxin BcIII. *Biochim. Biophys. Acta* **1764,** 1592–1600
7. Diochot, S., and Lazdunski, M. (2009) Sea anemone toxins affecting potassium channels. *Prog. Mol. Subcell. Biol.* **46,** 99–122
8. Diochot, S., Baron, A., Rash, L. D., Deval, E., Escoubas, P., Scarzello, S., Salinas, M., and Lazdunski, M. (2004) A new sea anemone peptide, APETx2, inhibits ASIC3, a major acid-sensitive channel in sensory neurons. *EMBO J.* **23,** 1516–1525
9. Catterall, W. A., Cestele, S., Yarov-Yarovoy, V., Yu, F. H., Konoki, K., and Scheuer, T. (2007) Voltage-gated ion channels and gating modifier toxins. *Toxicon* **49,** 124–141
10. Diochot, S., Loret, E., Bruhn, T., Beress, L., and Lazdunski, M. (2003) APETx1, a new toxin from the sea anemone *Anthopleura elegantissima*, blocks voltage-gated human ether-a-go-go-related gene potassium channels. *Mol. Pharmacol.* **64,** 59–69
11. Salceda, E., Garateix, A., Aneiros, A., Salazar, H., Lopez, O., and Soto, E. (2006) Effects of ApC, a sea anemone toxin, on sodium currents of mammalian neurons. *Brain Res.* **1110,** 136–143
12. Peigneur, S., Billen, B., Derua, R., Waelkens, E., Debaveye, S., Beress, L., and Tytgat, J. (2011) A bifunctional sea anemone peptide with Kunitz type protease and potassium channel inhibiting properties. *Biochem. Pharmacol.* **82,** 81–90
13. Bruhn, T., Schaller, C., Schulze, C., Sanchez-Rodriguez, J., Dannmeier, C., Ravens, U., Heubach, J. F., Eckhardt, K., Schmidtmayer, J., Schmidt, H., Aneiros, A., Wachter, E., and Beress, L. (2001) Isolation and characterisation of five neurotoxic and cardiotoxic polypeptides from the sea anemone *Anthopleura elegantissima*. *Toxicon* **39,** 693–702
14. Chagot, B., Diochot, S., Pimentel, C., Lazdunski, M., and Darbon, H. (2005) Solution structure of APETx1 from the sea anemone *Anthopleura elegantissima*: a new fold for an HERG toxin. *Proteins* **59,** 380–386
15. Zhang, M., Liu, X. S., Diochot, S., Lazdunski, M., and Tseng, G. N. (2007) APETx1 from sea anemone *Anthopleura elegantissima* is a gating modifier peptide toxin of the human ether-a-go-go- related potassium channel. *Mol. Pharmacol.* **72,** 259–268
16. Voilley, N., de Weille, J., Mamet, J., and Lazdunski, M. (2001) Nonsteroid anti-inflammatory drugs inhibit both the activity and the inflammation-induced expression of acid-sensing ion channels in nociceptors. *J. Neurosci.* **21,** 8026–8033
17. Price, M. P., McIlwrath, S. L., Xie, J., Cheng, C., Qiao, J., Tarr, D. E., Sluka, K. A., Brennan, T. J., Lewin, G. R., and Welsh, M. J. (2001) The DRASIC cation channel contributes to the detection of cutaneous touch and acid stimuli in mice. *Neuron* **32,** 1071–1083
18. Sluka, K. A., Price, M. P., Breese, N. M., Stucky, C. L., Wemmie, J. A., and Welsh, M. J. (2003) Chronic hyperalgesia induced by repeated acid injections in muscle is abolished by the loss of ASIC3, but not ASIC1. *Pain* **106,** 229–239
19. Deval, E., Noel, J., Lay, N., Alloui, A., Diochot, S., Friend, V., Jodar, M., Lazdunski, M., and Lingueglia, E. (2008) ASIC3, a sensor of acidic and primary inflammatory pain. *EMBO J.* **27,** 3047–3055
20. Karczewski, J., Spencer, R. H., Garsky, V. M., Liang, A., Leitl, M. D., Cato, M. J., Cook, S. P., Kane, S., and Urban, M. O. (2010) Reversal of acid-induced and inflammatory pain by the selective ASIC3 inhibitor, APETx2. *Br. J. Pharmacol.* **161,** 950–960
21. Blanchard, M. G., Rash, L. D., and Kellenberger, S. (2011) Inhibition of voltage-gated Na(+) currents in sensory neurons

by the sea anemone toxin APETx2. *Br J. Pharmacol.* **165,** 2167–2177
22. Ekberg, J., and Adams, D. J. (2006) Neuronal voltage-gated sodium channel subtypes: key roles in inflammatory and neuropathic pain. *Int. J. Biochem. Cell Biol.* **38,** 2005–2010
23. Jarvis, M. F., Honore, P., Shieh, C. C., Chapman, M., Joshi, S., Zhang, X. F., Kort, M., Carroll, W., Marron, B., Atkinson, R., Thomas, J., Liu, D., Krambis, M., Liu, Y., McGaraughty, S., Chu, K., Roeloffs, R., Zhong, C., Mikusa, J. P., Hernandez, G., Gauvin, D., Wade, C., Zhu, C., Pai, M., Scanio, M., Shi, L., Drizin, I., Gregg, R., Matulenko, M., Hakeem, A., Gross, M., Johnson, M., Marsh, K., Wagoner, P. K., Sullivan, J. P., Faltynek, C. R., and Krafte, D. S. (2007) A-803467, a potent and selective Nav1.8 sodium channel blocker, attenuates neuropathic and inflammatory pain in the rat. *Proc. Natl. Acad. Sci. U. S. A.* **104,** 8520–8525
24. Liu, M., and Wood, J. N. (2011) The roles of sodium channels in nociception: implications for mechanisms of neuropathic pain. *Pain Med.* **12**(Suppl. 3), S93–S99
25. Liman, E. R., Tytgat, J., and Hess, P. (1992) Subunit stoichiometry of a mammalian $K^+$ channel determined by construction of multimeric cDNAs. *Neuron* **9,** 861–871
26. Billen, B., Debaveye, S., Beress, L., Garateix, A., and Tytgat, J. (2010) Phyla- and subtype-selectivity of CgNa, a Na channel toxin from the venom of the giant caribbean sea anemone condylactis gigantea. *Front. Pharmacol.* **1,** 133
27. West, J. W., Patton, D. E., Scheuer, T., Wang, Y., Goldin, A. L., and Catterall, W. A. (1992) A cluster of hydrophobic amino acid residues required for fast Na(+)-channel inactivation. *Proc. Natl. Acad. Sci. U. S. A.* **89,** 10910–10914
28. Xiao, Y., Bingham, J. P., Zhu, W., Moczydlowski, E., Liang, S., and Cummins, T. R. (2008) Tarantula huwentoxin-IV inhibits neuronal sodium channels by binding to receptor site 4 and trapping the domain ii voltage sensor in the closed configuration. *J. Biol. Chem.* **283,** 27300–27313
29. Fozzard, H. A., and Lipkind, G. M. (2010) The tetrodotoxin binding site is within the outer vestibule of the sodium channel. *Mar. Drugs* **8,** 219–234
30. Van Der Haegen, A., Peigneur, S., and Tytgat, J. (2011) Importance of position 8 in mu-conotoxin KIIIA for voltage-gated sodium channel selectivity. *FEBS J.* **278,** 3408–3418
31. French, R. J., Yoshikami, D., Sheets, M. F., and Olivera, B. M. (2010) The tetrodotoxin receptor of voltage-gated sodium channels–perspectives from interactions with micro-conotoxins. *Mar. Drugs* **8,** 2153–2161
32. Campos, F. V., Chanda, B., Beirao, P. S., and Bezanilla, F. (2008) Alpha-scorpion toxin impairs a conformational change that leads to fast inactivation of muscle sodium channels. *J. Gen. Physiol.* **132,** 251–263
33. Stevens, M., Peigneur, S., and Tytgat, J. (2011) Neurotoxins and their binding areas on voltage-gated sodium channels. *Front. Pharmacol.* **2,** 71
34. Prikhod'ko, E. A., and Miller, L. K. (1999) The baculovirus PE38 protein augments apoptosis induced by transactivator IE1. *J. Virol.* **73,** 6691–6699
35. Peigneur, S., and Tytgat, J. (2012) The sophisticated peptide chemistry of venomous animals as a scource of novel insecticides acting upon voltage-gated sodium channels. In *Insecticides: Advances in Integrated Pest Management* (Perveen, F., ed), InTech, Rijeka, Croatia, http://cdn.intechweb.org/pdfs/25676.pdf
36. Swartz, K. J., and MacKinnon, R. (1997) Hanatoxin modifies the gating of a voltage-dependent K+ channel through multiple binding sites. *Neuron* **18,** 665–673
37. Phillips, L. R., Milescu, M., Li-Smerin, Y., Mindell, J. A., Kim, J. I., and Swartz, K. J. (2005) Voltage-sensor activation with a tarantula toxin as cargo. *Nature* **436,** 857–860
38. Redaelli, E., Cassulini, R. R., Silva, D. F., Clement, H., Schiavon, E., Zamudio, F. Z., Odell, G., Arcangeli, A., Clare, J. J., Alagon, A., de la Vega, R. C., Possani, L. D., and Wanke, E. (2010) Target promiscuity and heterogeneous effects of tarantula venom peptides affecting $Na^+$ and $K^+$ ion channels. *J. Biol. Chem.* **285,** 4130–4142
39. Liang, S. P., Zhang, D. Y., Pan, X., Chen, Q., and Zhou, P. A. (1993) Properties and amino acid sequence of huwentoxin-I, a neurotoxin purified from the venom of the Chinese bird spider *Selenocosmia huwena. Toxicon* **31,** 969–978
40. Peng, K., Shu, Q., Liu, Z., and Liang, S. (2002) Function and solution structure of huwentoxin-IV, a potent neuronal tetrodotoxin (TTX)-sensitive sodium channel antagonist from Chinese bird spider *Selenocosmia huwena. J. Biol. Chem.* **277,** 47564–47571
41. Wang, M., Rong, M., Xiao, Y., and Liang, S. (2011) The effects of huwentoxin-I on the voltage-gated sodium channels of rat hippocampal and cockroach dorsal unpaired median neurons. *Peptides* **34,** 19–25
42. Kozlov, S., and Grishin, E. (2011) The mining of toxin-like polypeptides from EST database by single residue distribution analysis. *BMC Genomics* **12,** 88
43. Rodriguez, A. A., Cassoli, J. S., Sa, F., Dong, Z. Q., de Freitas, J. C., Pimenta, A. M., de Lima, M. E., Konno, K., Lee, S. M., Garateix, A., and Zaharenko, A. J. (2011) Peptide fingerprinting of the neurotoxic fractions isolated from the secretions of sea anemones *Stichodactyla helianthus* and *Bunodosoma granulifera.* New members of the APETx-like family identified by a 454 pyrosequencing approach. *Peptides* **34,** 26–38
44. Diochot, S., Schweitz, H., Beress, L., and Lazdunski, M. (1998) Sea anemone peptides with a specific blocking activity against the fast inactivating potassium channel Kv3.4. *J. Biol. Chem.* **273,** 6744–6749
45. Liu, P., Jo, S., and Bean, B. P. (2012) Modulation of neuronal sodium channels by the sea anemone peptide BDS-I. *J. Neurophysiol.* **107,** 3155–3167
46. Xiao, Y., Jackson, J. O., 2nd, Liang, S., and Cummins, T. R. (2011) Common molecular determinants of tarantula huwentoxin-IV inhibition of Na+ channel voltage sensors in domains II and IV. *J. Biol. Chem.* **286,** 27301–27310

*Received for publication August 1, 2012.*
*Accepted for publication August 27, 2012.*